British Journal of Pharmacology

British Journal of Pharmacology (2016) **173** 2645–2656 2645

RESEARCH PAPER

Anti-angiogenic effects of novel cyclin-dependent kinase inhibitors with a pyrazolo[4,3-*d*]pyrimidine scaffold

Correspondence Professor Stefan Zahler, Department of Pharmacy – Center for Drug Research, Butenandtstr, 5-13, 81377 Munich, Germany. E-mail: stefan.zahler@cup.uni-muenchen.de

Received 23 March 2016; **Revised** 24 June 2016; **Accepted** 28 June 2016

S Zhang[1], M Ulrich[1], A Gromnicka[1], L Havlíček[2], V Kryštof[3], R Jorda[3], M Strnad[3], A M Vollmar[1] and S Zahler[1]

[1]Chair of Pharmaceutical Biology, Department of Pharmacy – Center for Drug Research, Ludwig-Maximilians-University, Munich, Germany, [2]Isotope laboratory, Institute of Experimental Botany ASCR, Prague, Czech Republic, and [3]Laboratory of Growth Regulators, Centre of the Region Haná for Biotechnological and Agricultural Research, Palacký University & Institute of Experimental Botany AS CR, Olomouc, Czech Republic

BACKGROUND AND PURPOSE

Cyclin-dependent kinase 5 (CDK5) has recently emerged as an attractive target in several tumour entities. Inhibition of CDK5 has been shown to have anti-angiogenic effects *in vitro* and *in vivo*. However, potent inhibitors of CDK5, which can be applied *in vivo*, are still scarce. We have recently developed a new series of 5-substituted 3-isopropyl-7-[4-(2-pyridyl)benzyl]amino-1(2)H-pyrazolo[4,3-*d*]pyrimidines that show a preference for inhibiting CDK5 and tested them *in vitro* and *in vivo* in a murine model of hepatocellular carcinoma.

EXPERIMENTAL APPROACH

All compounds were initially examined for effects on proliferation of HUVECs. The most potent compounds were then tested on migration, and one of them, LGR2674, was selected for assessing effects on nuclear fragmentation, cell cycle, cell viability and metabolic activity. Furthermore, LGR2674 was tested in a tube formation assay and *in vivo* in a murine model of hepatocellular carcinoma, induced by s.c. injection of HUH7 cells (measurement of *in vivo* toxicity, tumour vascularization, tumour cell proliferation and tumour size).

KEY RESULTS

LGR2674 showed an EC_{50} in the low nanomolar range in the proliferation and migration assays. Cytotoxic effects started at 50 nM, a concentration that did not influence the cell cycle. *In vivo,* LGR2674 was well tolerated and caused a clear reduction in vessel density in the tumours; also tumour cell proliferation was inhibited and tumour growth retarded.

CONCLUSIONS AND IMPLICATIONS

Pyrazolo[4,3-*d*]pyrimidine is a novel scaffold for the development of potent CDK inhibitors with *in vivo* potential. Such structures are good candidates for broadening our pharmacological arsenal against various tumours.

Abbreviations

CDK, cyclin-dependent kinase; HCC, hepatocellular carcinoma; SCID, severe combined immunodeficiency; SMA, smooth muscle actin

DOI:10.1111/bph.13546

Tables of Links

TARGETS	
Catalytic receptors[a]	**Enzymes**[b]
VEGF receptors	CDK5

LIGANDS
Roscovitine
Staurosporine

These Tables list key protein targets and ligands in this article which are hyperlinked to corresponding entries in http://www.guidetopharmacology.org, the common portal for data from the IUPHAR/BPS Guide to PHARMACOLOGY (Southan *et al.*, 2016) and are permanently archived in the Concise Guide to PHARMACOLOGY 2015/16 ([a,b]Alexander *et al.*, 2015a,b).

Introduction

The concept of starving a tumour by inhibiting its vascularization was initially developed by Judah Folkman (Folkman *et al.*, 1971); it is very intuitive, but has turned out not to be as easily achievable as initially hoped. In particular, the development of highly specific therapeutics, which selectively target the VEGF signalling pathway, like, for example, antibodies against VEGF or its receptor VEGFR-2, has revealed the 'behavioural plasticity' of tumours: they develop resistance by simply switching to different signalling pathways (e.g. FGF) (Dey *et al.*, 2015). As a consequence, the search for pharmacologically accessible targets against tumour angiogenesis is still, clinically, highly relevant.

One of these newly evolving targets is cyclin-dependent kinase 5 (CDK5), an atypical member of the family of CDKs (Liebl *et al.*, 2011a,b), which has only a minor impact on the cell cycle. CDK5 has been demonstrated to play a role in head and neck squamous carcinoma (Sun *et al.*, 2015), thyroid cancer (Pozo *et al.*, 2013; Pozo *et al.*, 2015) and hepatocellular carcinoma (HCC) (Ehrlich *et al.*, 2015) to name just a few. We have recently shown that CDK5 is important for lymph angiogenesis (Liebl *et al.*, 2015) and angiogenesis in general (Liebl *et al.*, 2010; Merk *et al.*, 2016) and that it can be influenced pharmacologically by small molecular inhibitors (Weitensteiner *et al.*, 2013). However, the potency, selectivity and clinical efficacy of CDK inhibitors are still an issue (Asghar *et al.*, 2015).

In the present work, we have investigated the *in vitro* effects (on functional aspects of endothelial cells) and *in vivo* applicability of novel inhibitors, 5-substituted 3-isopropyl-7-[4-(2-pyridyl)benzyl]amino-1(2)H-pyrazolo[4,3-*d*]pyrimidines) that have recently been shown to have an inhibitory preference for CDK5 (Vymetalova *et al.*, 2016), in a murine model of HCC.

Methods

Compounds

5-Substituted 3-isopropyl-7-[4-(2-pyridyl)benzyl]amino-1(2)H-pyrazolo[4,3-*d*]pyrimidines (Figure 1) were synthesized as described previously (Vymetalova *et al.*, 2016). For better cross reference, the same numbering of compounds has been displayed in Figure 1 as in the original article, in addition to an internal code (Laboratory of Growth Regulators (LGR) numbers). The structurally related CDK inhibitor CR8 was used as a control (Bettayeb *et al.*, 2008). The 10 mM stock solutions of the compounds were prepared in DMSO. The final DMSO concentrations did not exceed 0.1%, a concentration verified not to affect any of the experimental variables being studied.

Cell culture

HUVECs were obtained from PromoCell (Heidelberg, Germany). The culture medium used was an endothelial cell growth medium (PromoCell, Heidelberg, Germany), containing 10% heat inactivated fetal calf serum (FCS) and supplemented with a mix of vitamins and growth factors (PromoCell, Heidelberg, Germany). Culture dishes were routinely coated with collagen. HUH7 cells were obtained from the Japanese Collection of Research Bioresources and validated by the Deutsche Sammlung von Mikroorganismen und Zellkulturen in Braunschweig, Germany. HUH7 cells were cultivated in DMEM containing 10% FCS. Cells were incubated at 37°C and 5% CO_2.

Proliferation assay

The proliferation assay was performed as described previously (Rath *et al.*, 2012). Briefly, 1500 HUVECs per well were seeded into 96-well plates in 100 μL of media. After 24 h, one plate of control cells was fixed and stained with crystal violet (see below) to determine the initial cell number. The other plates were incubated with increasing concentrations of the compounds to be tested for 72 h. After this time, cells were stained with crystal violet solution (0.5% crystal violet in 20% methanol) for 10 min. Free crystal violet was removed by rinsing with distilled water, and cells were subsequently air dried. Crystal violet, which mainly binds to DNA, was eluted from cells with 0.1 M sodium citrate in 50% ethanol. The absorbance of crystal violet is proportional to the cell number and was determined at 540 nm with Magellan six-plate reader (TECAN, Männedorf, Switzerland). GRAPHPAD PRISM (GraphPad Software, La Jolla, CA, USA) was used to obtain and to calculate the EC_{50} values for each compound using a nonlinear regression curve fit. Three independent experiments were performed with each compound and included six replicates.

Migration (scratch assay)

HUVECs were seeded into 24-well plates and grown to confluency. A wound of approximately 1 mm was imposed on the monolayers by scratching them with a custom-made device. Detached cells were removed by washing with PBS; remaining cells then were incubated for 16 h in starvation medium (free of growth factors and serum, 0% migration), culture medium (100% migration) or culture

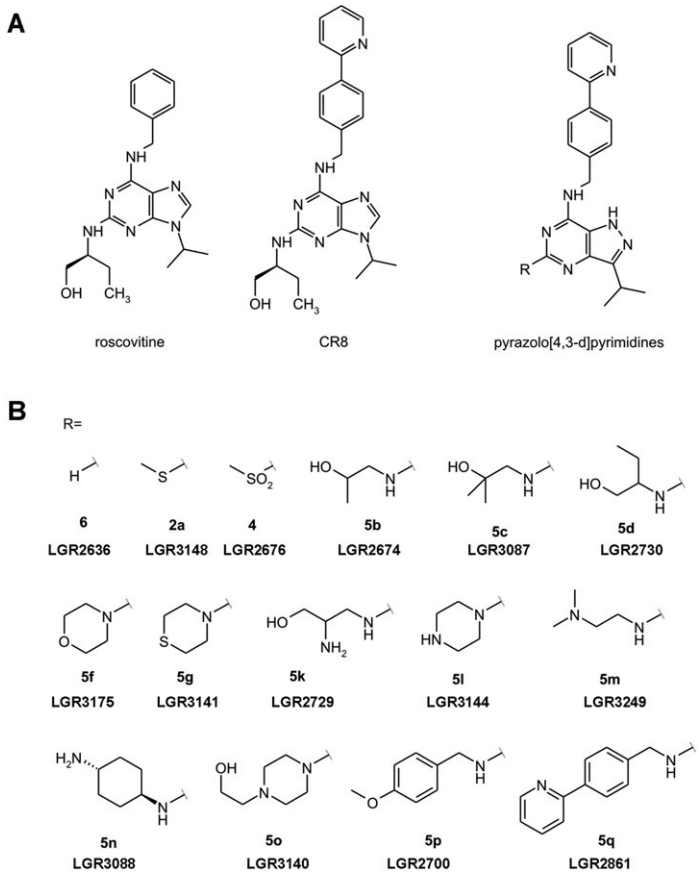

Figure 1

(A) Chemical structure of roscovitine, the previously published derivative CR8 and the pyrazolo[4,3-*d*]pyrimidine scaffold used. (B) Chemical structures of the substituents (*R*). The LGR numbering is an internal code. For better cross reference to the manuscript describing their synthesis (Vymetalova *et al.*, 2016), the original compound numbers from that publication are also provided.

medium containing increasing concentrations of the test compounds. Cells were washed with PBS after incubation and then fixed with 4% formaldehyde. One image was taken of each well (centre position) on an inverted light microscope (Axiovert 200; Zeiss, Jena, Germany) with a 5× lens using an Imago-QE camera system and the appending software (Till Photonics, Gräfelfing, Germany). For quantification, these images were analysed with IMAGEJ. Migration was calculated relative to control and to starvation control. In previous experiments, we had determined that cell proliferation does not contribute to wound closure in this setting by using mitomycin (Liebl *et al.*, 2010). Data are means ± SEM of at least three independent experiments, each performed in triplicate.

Detection and quantification of nuclear fragmentation and cell cycle

HUVECs were mixed with test compounds and seeded on 24-well plates for 24 h and 48 h respectively. Quantification of nuclear fragmentation was performed according to Nicoletti (Nicoletti *et al.*, 1991).

After being treated, HUVECs were harvested on ice and incubated in a hypotonic buffer (0.1% sodium citrate, 0.1% Triton X-100 and 50 $\mu g \cdot mL^{-1}$ propidium iodide) overnight at 4°C and then analysed by flow cytometry on a FACSCalibur (Becton Dickinson, Heidelberg, Germany) using CELLQUEST PRO software (Becton Dickinson, Heidelberg, Germany). Nuclei to the left of the G1-peak containing hypodiploid DNA were considered as fragmented. In the same set of experiments, the percentage of living cells in G0/G1, S and G2/M phase was evaluated after gating out cell debris, using the Watson pragmatic model for cell cycle analysis in the FLOWJO software (Tree Star Inc., Ashland, OR, USA). All experiments were performed in triplicate and each experiment was repeated five times (n = 5).

Measurement of cell viability

To detect membrane integrity as a sign of cellular viability, a trypan blue exclusion assay was performed. Cells were cultivated until reaching full or 50% confluency, treated with the compound of interest at different concentrations for 24 h, and then detached with trypsin/EDTA. Trypsin was inactivated with serum, and the cell suspension injected into a cell counter (ViCell, Beckmann Coulter, Krefeld, Germany), which automatically adds trypan blue and detects cells that have taken up the dye. All experiments were performed in triplicate and each experiment was repeated five times (n = 5).

Measurement of metabolic activity

To further characterize the functional state of the treated cells, we measured metabolic activity using the CellTiter-Blue kit from Promega (Mannheim, Germany). Cells were cultivated until reaching full or 50% confluency and treated with compound at the respective concentration for 24 h. The assay was performed according to the manufacturer's instructions. All experiments were performed in triplicate and each experiment was repeated five times (n = 5).

Tube formation

A total of 10 000 HUVEC cells were seeded on matrigel (Matrigel™, Schubert & Weiss-OMNILAB, Munich, Germany) in an angiogenesis slide from Ibidi (Munich, Germany), treated as indicated and incubated for 20 h. Images were taken using a TILLvisION system. Analysis of images was performed by Wimasis GmbH (Munich, Germany). As parameters of tube formation tube length (arithmetic mean of the individual tube lengths), number of branches (the branching points are parts of the skeleton where three or more tubes converge), number of loops [a loop is an area of the background enclosed (or almost) by the tubular structure] and number of nets (a net is an isolated region of tubes that contains, at least, one branching point) were used. The experiments were repeated five times (n = 5), each done in triplicate.

Subcutaneous murine tumour xenograft model

Mice with severe combined immunodeficiency (SCID mice) are commonly used as a standard model for ectopic tumours induced by the s.c. injection of human cells. HUH7 cells have been repeatedly used in this context and provide well vascularized tumours, which are appropriate for studying effects on tumour angiogenesis. A total of 20 female SCID mice were chosen for the *in vivo* experiments. This albino immunodeficient strain (CB17/lcr-Prkdcscid/Crl) was ordered from Charles River Laboratories (Sulzfeld, Germany). All laboratory mice were purchased at an age of 5 weeks, and were first used for the experiment when they were 6-weeks-old to give them enough time to adapt to the new housing conditions. At the beginning of the trial, the weights of the mice ranged between 15.5 and 18.9 g.

Mice were housed in a special air-conditioned room within individual ventilated cages (type II long, Tecniplast). They were subjected to a 12 h day and night cycle and had *ad libitum* access to autoclaved water (in bottles) and autoclaved standard food (producer: Sniff). The occupancy was five animals per cage. The cages, inclusive litter and bedding inlets, were changed once a week.

The left flanks of all 20 SCID mice were shaved before cell inoculation. Each mouse was inoculated with 3×10^6 HUH7 cells dissolved in 100 µL PBS, given by s.c. injection into the left flank by use of 1 mL syringes in combination with 27 gauge (G) needles.

Tumour-bearing mice were randomly divided into two groups, one control group (n = 10) and an LGR2674 treatment group (n = 10). The control group was treated daily with vehicle, while the other group received, daily, LGR2674 at a dose of 1.5 $mg \cdot kg^{-1}$ dissolved in 5% DMSO, 10% solutol and 85% PBS. Therapy started on day 8 after tumour cell inoculation. Mice received their daily i.p. injection 13 times (d8, d9, d10, d11, d12, d13, d14, d15, d16, d17, d18, d19 and d20). One mouse from the control group and one mouse from the LGR2674-treated group had to be taken out of the experiment on day 17 because the volume of their tumour exceeded 1000 mm^3. The final day for the other animals was day 20. Mice were killed by cervical dislocation. Solid tumours were removed, weighed, photographed and split into two parts, one part was stored at −80°C and the other was preserved in 1% paraformaldehyde (PFA).

The general condition of the mice was evaluated by assessing and applying a score to their breathing, behaviour, posture, weight and body condition; signs of pain were identified as bent position, closed eyes and isolation from the group and by changes to their fur and colour of the skin and mucosa (eyes and anus).

All *in vivo* experiments were performed according to the legal terms for animal experiments of the local administration (Government of Upper Bavaria). Animal studies are reported in compliance with the ARRIVE guidelines (Kilkenny *et al.*, 2010; McGrath & Lilley, 2015).

Immunofluorescence

Paraffin sections from each group were deparaffinized in xylene (5 min) and rehydrated through descending concentrations of ethanol (10 min in 100% and 10 min in 95%). Before immunohistochemical staining, antigen retrieval was performed by boiling the sections in sodium citrate buffer (10 mM sodium citrate, 0.05% Tween 20, pH 6.0) for 20 min. After blocking for 1 h in 1% BSA (in PBS), the slides were incubated with primary antibody [mouse anti α smooth muscle actin (SMA), CY3 labelled, Sigma-Aldrich c-6198, rat anti CD31, Dianova DIA-310, and rabbit anti Ki67, Abcam ab15580] in 1% BSA 1:200 for 1 h and subsequently washed three times with PBS (5 min). After incubation with the secondary antibody (Alexa Fluor 647, chicken anti-rabbit IgG, and Alexa Fluor 488, goat anti-rat IgG, both from Thermo Scientific) in 1% BSA 1:400, three washing steps with PBS followed.

Four high power (40×) images were obtained (image area 0.0355 mm^2) per slide with a Leica SP8 SMD confocal microscope for determination of vessel density and number of Ki67 positive nuclei.

Western blot

Tissues were lysed, and proteins separated by SDS-PAGE. After blotting to a nitrocellulose membrane, phosphorylated Ser/Thr-Pro motifs were detected by a specific antibody (MPM-2, Cat.#05-368, Millipore, Darmstadt, Germany). Ser/Thr-Pro is a CDK5 phosphorylation motif, and this antibody has been used for the purpose of detecting CDK5 activity previously (Pareek *et al.*, 2010). Chemiluminescence detection was done on a ChemiDoc system (BioRad, Munich, Germany); loading of the lanes was normalized using the stain-free technology according to the manufacturer's instructions.

Statistical analysis

The data and statistical analysis comply with the recommendations on experimental design and analysis in pharmacology (Curtis *et al.*, 2015).

SIGMAPLOT software with Sigma Stat integration (Systat, Erkrath, Germany) was used for most statistical calculations. The dose response curves were calculated as sigmoidal nonlinear fit, and EC_{50} values calculated using GRAPHPAD PRISM software. For comparison of two groups, an unpaired *t*-test was performed. Three or more groups were compared by one-way ANOVA, followed by multiple comparisons versus control (Dunnett's test). All data are expressed as means ± SEM. Differences between groups were deemed statistically different at $P < 0.05$ and indicated by an asterisk.

Blinding

All data were evaluated by a blinded analyst.

Results

Inhibition of HUVEC proliferation

We initially tested, whether, and at which concentrations the compounds inhibited endothelial cell proliferation. All compounds were active at a range between low nanomolar and low micromolar concentrations (Figure 2A). For the four compounds, which displayed a pronounced inhibition at 100 nM, detailed dose-response curves were obtained and they were shown to have EC_{50} values between 20 and 37 nM (Figure 2B). These four most potent compounds (LGR2674, LGR2730, LGR3087 and LGR3144) were selected for further testing.

Inhibition of cell migration

In the scratch assay, the four selected compounds inhibited migration of HUVECs with very similar potencies (EC_{50} values ranging from 22 to 39 nM, Figure 3A). Figure 3B shows representative images of the scratch assays. Because the potencies of the four compounds were in the same range, the technical criterion for the selection of LGR2674 for further studies was its good preference towards CDK5 (Vymetalova *et al.*, 2016) and its easier synthetic accessibility.

Effects of LGR2674 on nuclear fragmentation, cell cycle, cell viability and metabolic activity

Measurement of nuclear fragmentation (sub G1 DNA, which mainly occurs during apoptotic cell death) showed that LGR2674 had no cytotoxic effects up to 30 nM, while 100 nM caused pronounced effects (Figure 4A). Cell cycle analysis (Figure 4B) showed that even at a cytotoxic concentration of 100 nM, no shift in the cell cycle phases occurs. This indicates that the inhibition of cell cycle relevant CDKs (e.g. CDK1 or 2) does not contribute to the functional effects of LGR2674. In a trypan blue exclusion assay, cells stay intacted below a concentration of 50 nM in confluent (Figure 4C, left panel), as well as in proliferating cells (Figure 4C, right panel). Metabolic activity was not influenced in confluent cells over the concentration range tested (Figure 4D, left panel), while it started to diminish at 30 nM in proliferating cells (Figure 4D, right panel). In the range concentrations where migration was impaired, a contribution of cytotoxicity to this inhibitory effect can only be minimal.

Inhibition of tube formation by LGR2674

In a tube formation assay on Matrigel, LGR2674 clearly altered the structure of the endothelial networks (Figure 5A). Although the nominal tube length and the degree of branching were only slightly reduced (Figure 5B), the integrity of the network was largely damaged starting at 35 nM, as indicated by a reduction in the number of closed loops and an increase in the number of independent nets, which are no longer integral (Figure 5C).

Inhibition of tumour vascularization, tumour cell proliferation and tumour growth by LGR2674

Injection, i.p., of mice with LGR2674 significantly reduced the tumour burden of the mice (Figure 6A). The treatment caused a weight loss of about 18% (Figure 6B), but was otherwise well tolerated (absence of signs of distress, like altered breathing, behaviour, posture, signs of pain as a bent position, closed eyes and isolation from the group and by changes in their fur and colour of the skin and mucosa). The number of Ki67 positive nuclei (i.e. proliferating cells) was significantly lower in the treatment group as compared with controls (Figure 6C). In order to get an impression of whether the inhibitor directly reduces CDK5 activity in tumour cells *in vivo*, we performed a Western blot for phosphorylated CDK5 consensus motifs. It has, however, to be kept in mind that phosphorylation motifs are not specific for one single kinase. In the case of CDK5, there is a considerable overlap with, for example, ERK1, GSK-3. The band density in the lysates from treated animals was significantly lower than in controls, suggesting an inhibition of CDK5 (Figure 6D). Analysis of vascular density with two different vascular markers (αSMA and CD31) showed reduced vascularization of the tumours in treated animals (Figure 6E).

Discussion

Since their discovery as the main regulators of cell cycle progression in the early 1980s, and due to the observation that they are often dysregulated in tumours (Asghar *et al.*, 2015), CDKs have received continuous interest as pharmacological targets. The CDK inhibitors that were first described, such as olomoucine (Glab *et al.*, 1994; Vesely *et al.*, 1994) and roscovitine (De Azevedo *et al.*, 1997), had a low potency and selectivity. Ever since, as with other families of kinase inhibitors, there has been a quest for compounds with increased potency and selectivity. However, during the past few years, the paradigm of obtaining highly selective kinase inhibitors for clinical use has been questioned (Faivre *et al.*, 2006; Zimmermann *et al.*, 2007; Wesierska-Gadek and Krystof, 2009). So, instead of searching for compounds with maximum selectivity, another approach to speed up drug development is to identify drugs with the desired functional properties by phenotypic screening (MacDonald *et al.*, 2006). This is particularly important for CDK inhibitors, because CDKs are involved in various heterogeneous biological activities, ranging from cell proliferation and migration to metabolism, and in the case of CDK5 even to cognitive processes (Liebl *et al.*, 2011a,b).

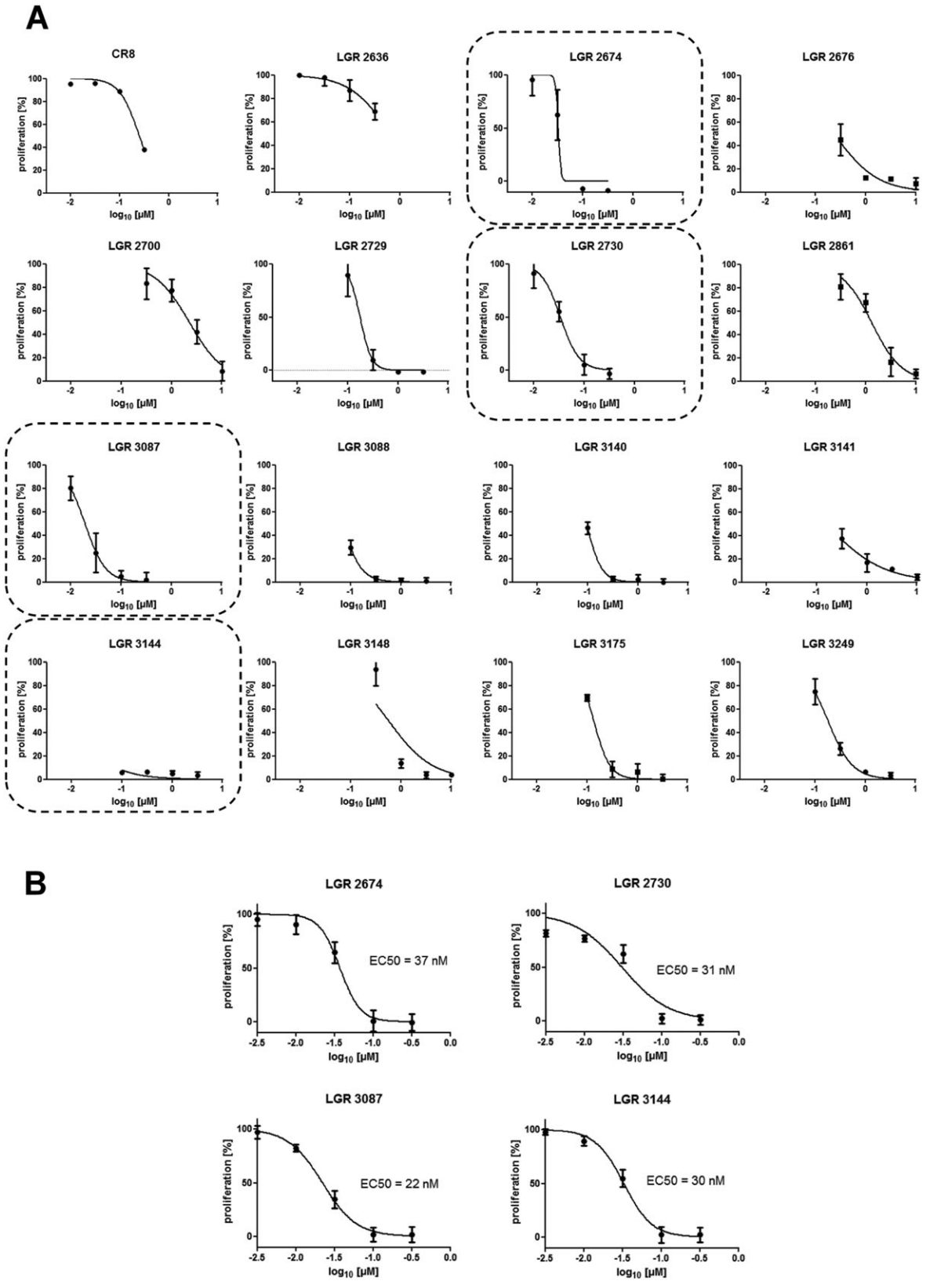

Figure 2

(A) All the derivatives tested inhibit endothelial cell proliferation in a dose-dependent manner. (B) The four most potent compounds were selected for generating detailed dose-response curves and for calculating EC_{50} values. Data are presented as means ± SEM of three independent experiments performed with six replicates in each.

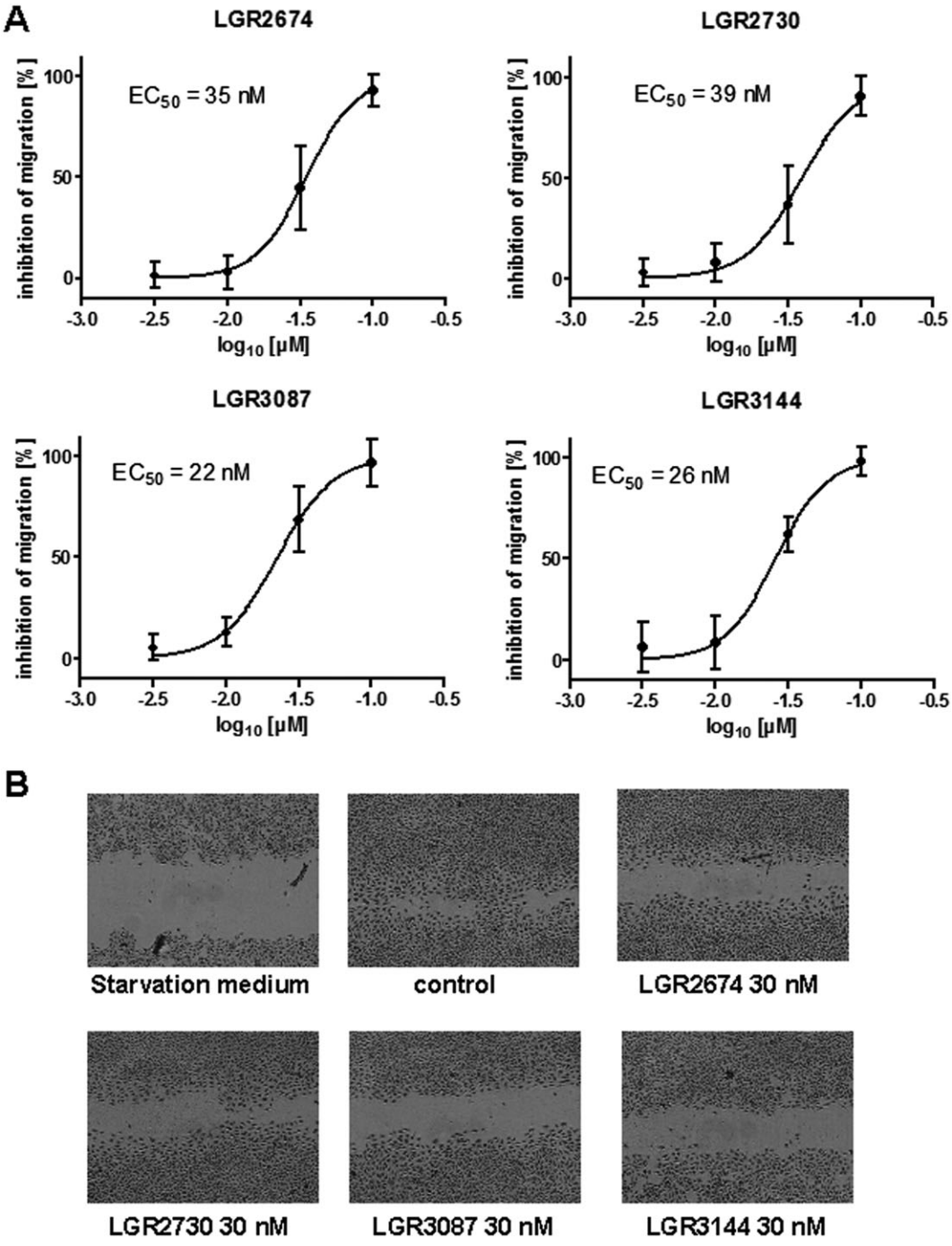

Figure 3

(A) The four selected compounds inhibited endothelial cell migration in the scratch assay dose-dependently with similar potency (EC_{50} approximately 30 nM). (B) Representative images of scratch assays. Data are means ± SEM of three independent experiments (n = 3), each performed in triplicate.

Because we have identified CDK5 as an important regulator of both lymphangiogenesis and angiogenesis (Liebl *et al.*, 2010; Liebl *et al.*, 2015; Merk *et al.*, 2016), we utilized a combination of *in vitro* parameters for phenotypic screening, which indicate the anti-angiogenic potential of a CDK inhibitor: a reduction in endothelial cell proliferation and migration, and a prevalence for inhibiting CDK5 and CDK2 over other CDKs (Liebl *et al.*, 2011a,b; Weitensteiner *et al.*, 2013). Following this workflow, we have screened a series of 16 recently prepared 5-substituted 3-isopropyl-7-[4-(2-pyridyl)benzyl]amino-1(2)H-pyrazolo[4,3-*d*]pyrimidines (Vymetalova *et al.*, 2016) and were able to select four promising candidates, with about a 1000-fold increased potency in cellular assays, as

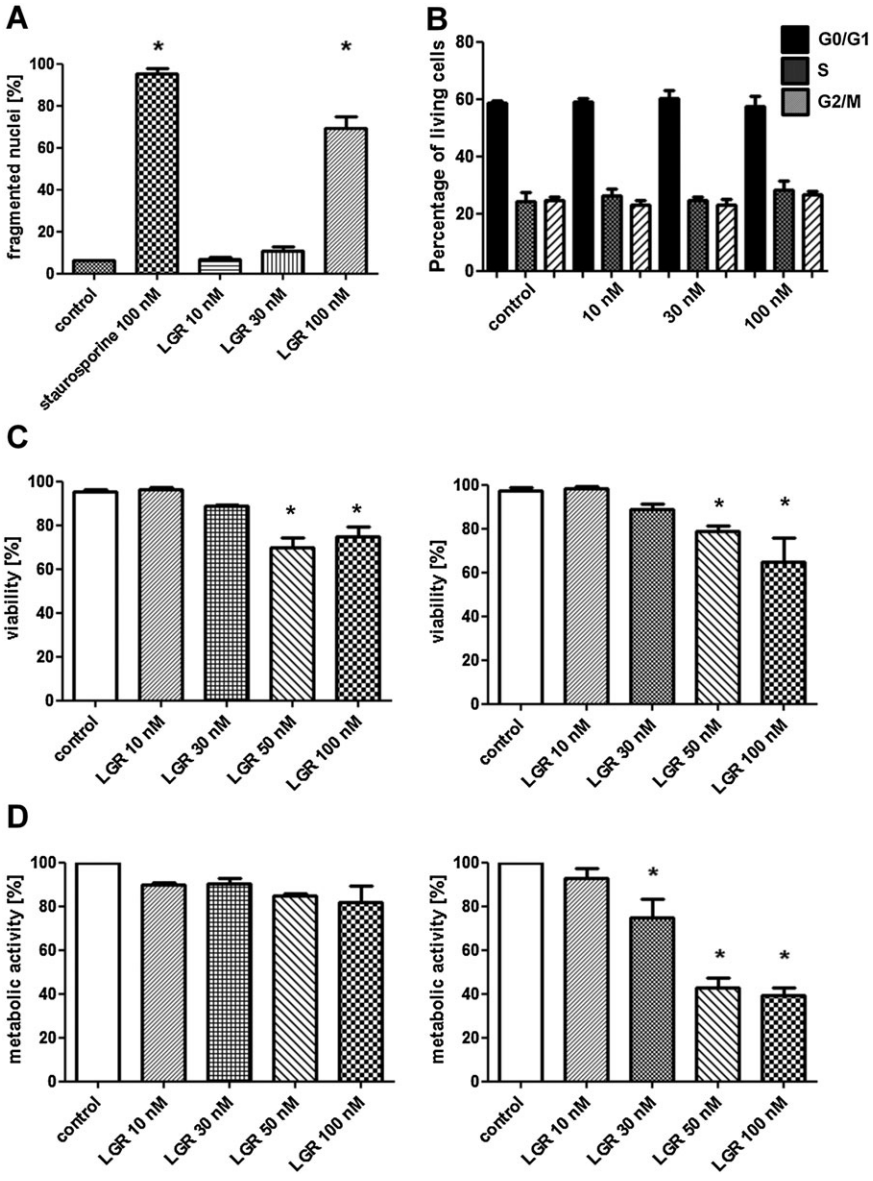

Figure 4

(A) At a concentration that reduced migration (30 nM), LGR2674 did not cause nuclear fragmentation as determined by flow cytometry. (B) The cell cycle was not altered even at a concentration that caused marked nuclear fragmentation (100 nM), arguing against pronounced effects on CDKs relevant for cell cycle progression. (C) Cell viability as measured by trypan blue exclusion was not significantly altered at 30 nM in both confluent (left panel) and proliferating cells (right panel). (D) Metabolic activity as measured by the CellTiter-Blue assay was not influenced in confluent cells at any concentration tested (left panel), but started to drop at 30 nM in proliferating cells (right panel). Data are means ± SEM of five independent experiments ($n = 5$), each performed in triplicate. *$P < 0.05$, significantly different from controls.

compared with the standard compound roscovitine. Three of these compounds were relatively selective for CDK5 (Vymetalova *et al.*, 2016). For reasons of synthetic accessibility, which is an important issue when a compound has to be synthesized on a medium scale, we continued further testing with LGR2674 in assays on cell viability, metabolic activity, tube formation and in a murine model of HCC. In the tube formation assay, LGR2674 concentration-dependently caused a fragmented phenotype of network formation. The tests on metabolic activity showed that proliferating cells are more susceptible to treatment than confluent cells. This might mean that the resting endothelium outside the tumour resists treatment much better than the activated endothelium in growing tumour vessels. *In vivo*, tumour growth was reduced to a similar extent as tumour cell proliferation. LGR2674 reduced the vascularization of the tumours. Interestingly, the reduction in αSMA, a vascular smooth muscle marker, was less pronounced than that of CD31, an endothelial marker, which might indicate that endothelial cells are particularly sensitive to the effects of this compound. Although LGR2674 did not inhibit the cell cycle *in vitro* at the concentrations used, it did reduce the number of actively

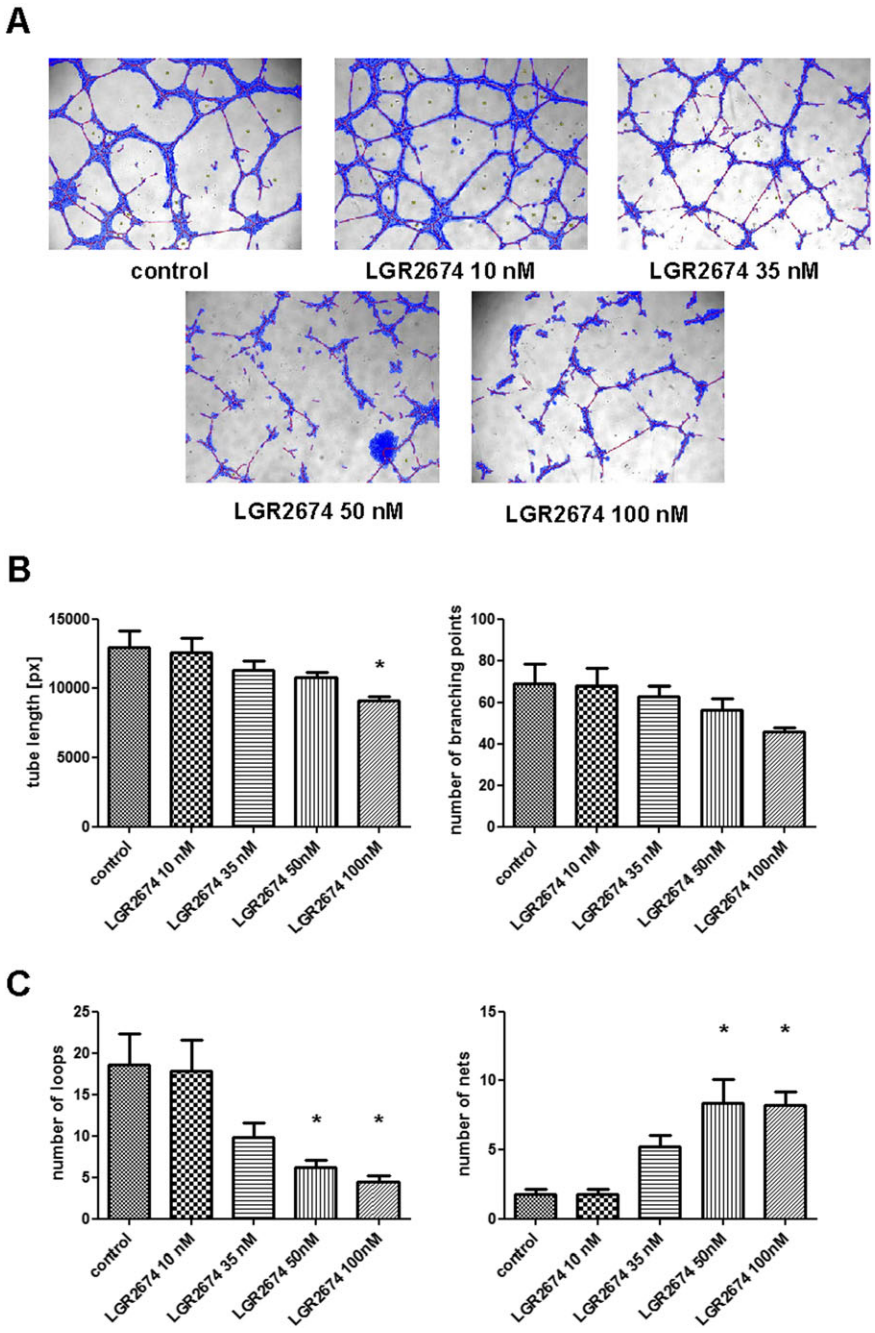

Figure 5

(A) Representative images of tube formation before and after treatment with LGR2674. (B) Tube length (left panel) and number of branches (right panel) were only reduced to a minor degree. (C) Parameters indicating the structural complexity of the networks formed and their fragmentation, like number of closed loops (left panel) or number of independent nets (right panel), were significantly reduced by LGR2674. The experiments were repeated five times ($n = 5$), each in triplicate. *$P < 0.05$, significantly different from controls.

proliferating tumour cells in the *in vivo* model. This could result from it only targeting cell cycle CDKs and/or from an indirect effect: tumour cell proliferation might decrease due to a reduced supply of metabolites after inhibition of angiogenesis. This might also explain why the effect on angiogenesis is clearer than that on tumour growth as such.

One important issue that needed to be addressed was the pharmacokinetics of the drug in the organism, as well as the proof of principle that the expected mode of action (inhibition of CDK5 activity) actually takes place *in vivo*. Because we have no analytics of appropriate sensitivity at hand to study the concentrations of LGR2674 in plasma of the treated animals, we looked for an indicator of enzymatic activity of CDK5 in the tumour tissue. Indeed, LGR2674 reduced the phosphorylation of CDK5 substrate motifs in the tumours of treated animals.

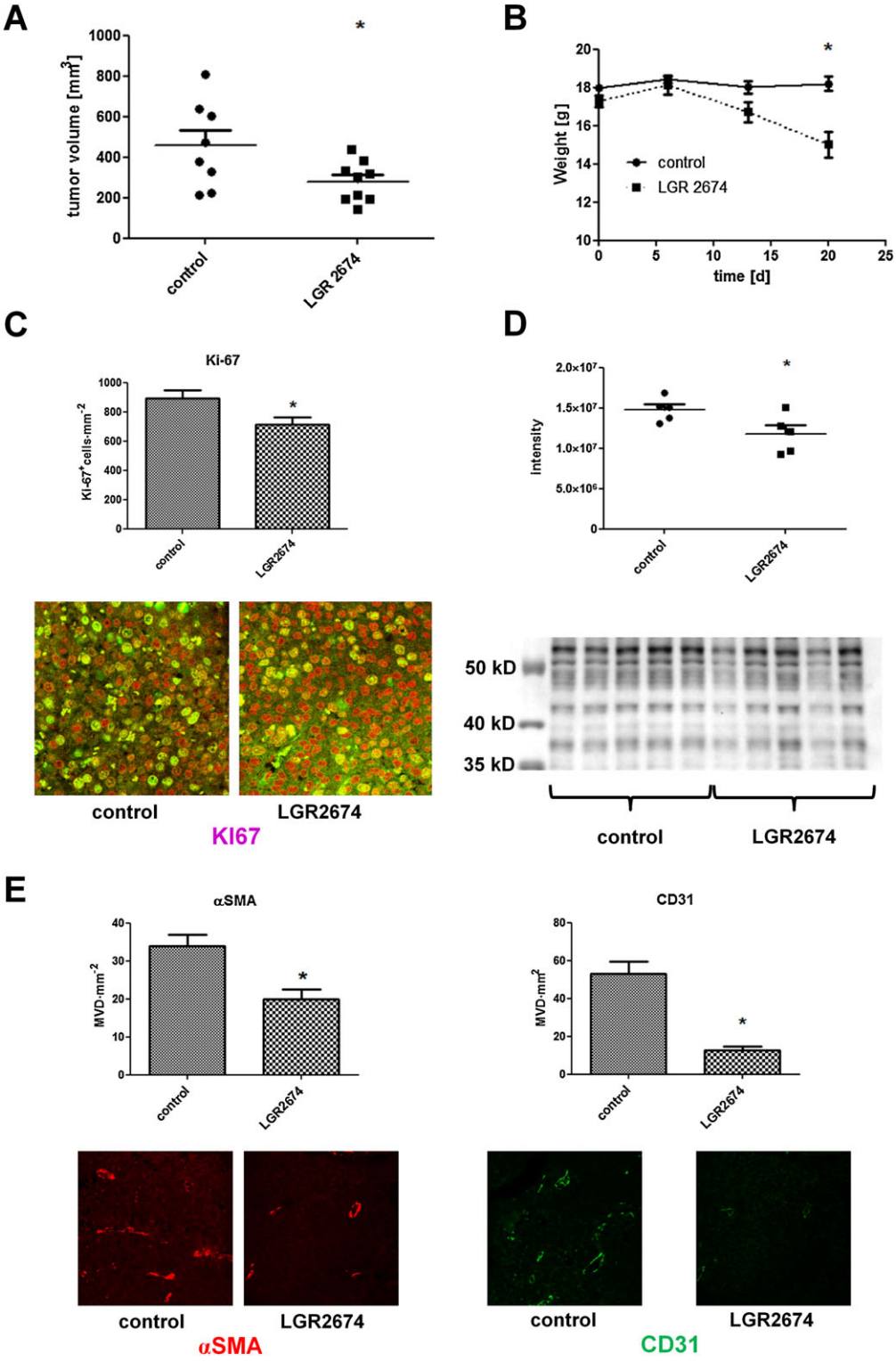

Figure 6

(A) Tumour growth was significantly reduced by treatment with LGR2674. (B) LGR2674 was tolerated reasonably well in mice after an i.p. injection of 0.03 mg·kg^{-1} day^{-1}, but caused a weight loss of approximately 18% over the course of the experiment. (C) The number of nuclei positive for the proliferation marker Ki67 was significantly reduced in tumour tissue from treated mice (upper panel). Lower panel: representative images from control mice and mice treated with LGR2674. Nuclei are stained red, Ki67 in green. Ki67 positive nuclei appear yellow in the overlay image. (D) Western blot for phosphorylated CDK5 substrate motifs. Upper panel: quantification of the band intensity up to a size marker of 70 kD. The treated animals show a lower degree of phosphorylation. Lower panel: chemiluminescence image of the blot. (E) Tumour vascularization was significantly reduced in treated animals, as shown by histological quantification of two independent vessel markers (αSMA, left panel and CD31, right panel). *$P < 0.05$, significantly different from controls.

In summary, we have identified 5-substituted 3-isopropyl-7-[4-(2-pyridyl)benzyl]amino-1(2)H-pyrazolo[4,3-*d*]pyrimidines as a promising scaffold for the development of novel CDK inhibitors with anti-angiogenic properties. These might help us to overcome issues of therapy resistance against the established VEGF-centred inhibitors of angiogenesis.

Acknowledgements

This work was in part supported by the German Research Council (DFG) project ZA 186/7-1 and the Grant Agency of the Czech Republic (no. 14-19590S). The expert technical assistance of Jana Peliskova is gratefully acknowledged.

Author contributions

S.Z., M.U. and A.G. performed the experiments and contributed to data analysis, L.H.,V.K., R.J. and M.S. developed the compounds and A.M.V. and S.Z. conceived and supervised the project and wrote the manuscript.

Conflict of interest

The authors declare no conflicts of interest.

Declaration of transparency and scientific rigour

This Declaration acknowledges that this paper adheres to the principles for transparent reporting and scientific rigour of preclinical research recommended by funding agencies, publishers and other organisations engaged with supporting research.

References

Alexander SPH, Fabbro D, Kelly E, Marrion N, Peters JA, Benson HE *et al.* (2015a). The Concise Guide to PHARMACOLOGY 2015/16: Catalytic receptors. Br J Pharmacol 172: 5979–6023.

Alexander SPH, Fabbro D, Kelly E, Marrion N, Peters JA, Benson HE *et al.* (2015b). The Concise Guide to PHARMACOLOGY 2015/16: Enzymes. Br J Pharmacol 172: 6024–6109.

Asghar U, Witkiewicz AK, Turner NC, Knudsen ES (2015). The history and future of targeting cyclin-dependent kinases in cancer therapy. Nat Rev Drug Discov 14: 130–146.

Bettayeb K, Oumata N, Echalier A, Ferandin Y, Endicott JA, Galons H *et al.* (2008). CR8, a potent and selective, roscovitine-derived inhibitor of cyclin-dependent kinases. Oncogene 27: 5797–5807.

Curtis MJ, Bond RA, Spina D, Ahluwalia A, Alexander SP, Giembycz MA *et al.* (2015). Experimental design and analysis and their reporting: new guidance for publication in BJP. Br J Pharmacol 172: 3461–3471.

De Azevedo WF, Leclerc S, Meijer L, Havlicek L, Strnad M, Kim SH (1997). Inhibition of cyclin-dependent kinases by purine analogues: crystal structure of human cdk2 complexed with roscovitine. Eur J Biochem 243: 518–526.

Dey N, De P, Brian LJ (2015). Evading anti-angiogenic therapy: resistance to anti-angiogenic therapy in solid tumors. Am J Transl Res 7: 1675–1698.

Ehrlich SM, Liebl J, Ardelt MA, Lehr T, De Toni EN, Mayr D *et al.* (2015). Targeting cyclin dependent kinase 5 in hepatocellular carcinoma - a novel therapeutic approach. J Hepatol 63: 102–113.

Faivre S, Djelloul S, Raymond E (2006). New paradigms in anticancer therapy: targeting multiple signaling pathways with kinase inhibitors. Semin Oncol 33: 407–420.

Folkman J, Merler E, Abernathy C, Williams G (1971). Isolation of a tumor factor responsible for angiogenesis. J Exp Med 133: 275–288.

Glab N, Labidi B, Qin LX, Trehin C, Bergounioux C, Meijer L (1994). Olomoucine, an inhibitor of the cdc2/cdk2 kinases activity, blocks plant cells at the G1 to S and G2 to M cell cycle transitions. FEBS Lett 353: 207–211.

Kilkenny C, Browne W, Cuthill IC, Emerson M, Altman DG (2010). Animal research: reporting *in vivo* experiments: the ARRIVE guidelines. Br J Pharmacol 160: 1577–1579.

Liebl J, Furst R, Vollmar AM, Zahler S (2011a). Twice switched at birth: cell cycle-independent roles of the "neuron-specific" cyclin-dependent kinase 5 (Cdk5) in non-neuronal cells. Cell Signal 23: 1698–1707.

Liebl J, Krystof V, Vereb G, Takacs L, Strnad M, Pechan P *et al.* (2011b). Anti-angiogenic effects of purine inhibitors of cyclin dependent kinases. Angiogenesis 14: 281–291.

Liebl J, Weitensteiner SB, Vereb G, Takacs L, Furst R, Vollmar AM *et al.* (2010). Cyclin-dependent kinase 5 regulates endothelial cell migration and angiogenesis. J Biol Chem 285: 35932–35943.

Liebl J, Zhang S, Moser M, Agalarov Y, Demir CS, Hager B *et al.* (2015). Cdk5 controls lymphatic vessel development and function by phosphorylation of Foxc2. Nat Commun 6: 7274. doi: 10.1038/ncomms8274.

MacDonald ML, Lamerdin J, Owens S, Keon BH, Bilter GK, Shang Z *et al.* (2006). Identifying off-target effects and hidden phenotypes of drugs in human cells. Nat Chem Biol 2: 329–337.

McGrath JC, Lilley E (2015). Implementing guidelines on reporting research using animals (ARRIVE etc.): new requirements for publication in BJP. Br J Pharmacol 172: 3189–3193.

Merk H, Zhang S, Lehr T, Muller C, Ulrich M, Bibb JA *et al.* (2016). Inhibition of endothelial Cdk5 reduces tumor growth by promoting non-productive angiogenesis. Oncotarget 7: 6088–6104.

Nicoletti I, Migliorati G, Pagliacci MC, Grignani F, Riccardi C (1991). A rapid and simple method for measuring thymocyte apoptosis by propidium iodide staining and flow cytometry. J Immunol Methods 139: 271–279.

Pareek TK, Lam E, Zheng X, Askew D, Kulkarni AB, Chance MR *et al.* (2010). Cyclin-dependent kinase 5 activity is required for T cell activation and induction of experimental autoimmune encephalomyelitis. J Exp Med 207: 2507–2519.

Pozo K, Castro-Rivera E, Tan C, Plattner F, Schwach G, Siegl V *et al.* (2013). The role of Cdk5 in neuroendocrine thyroid cancer. Cancer Cell 24: 499–511.

Pozo K, Hillmann A, Augustyn A, Plattner F, Hai T, Singh T *et al.* (2015). Differential expression of cell cycle regulators in CDK5-dependent medullary thyroid carcinoma tumorigenesis. Oncotarget 6: 12080–12093.

Rath S, Liebl J, Furst R, Ullrich A, Burkhart JL, Kazmaier U *et al.* (2012). Anti-angiogenic effects of the tubulysin precursor pretubulysin and of simplified pretubulysin derivatives. Br J Pharmacol 167: 1048–1061.

Southan C, Sharman JL, Benson HE, Faccenda E, Pawson AJ, Alexander SP *et al.* (2016). The IUPHAR/BPS Guide to PHARMACOLOGY in 2016: towards curated quantitative interactions between 1300 protein targets and 6000 ligands. Nucl Acids Res 44: D1054–D1068.

Sun SS, Zhou X, Huang YY, Kong LP, Mei M, Guo WY*et al.* (2015). Targeting STAT3/miR-21 axis inhibits epithelial-mesenchymal transition via regulating CDK5 in head and neck squamous cell carcinoma. Mol Cancer 14: 213.

Vesely J, Havlicek L, Strnad M, Blow JJ, Donella-Deana A, Pinna L *et al.* (1994). Inhibition of cyclin-dependent kinases by purine analogues. Eur J Biochem 224: 771–786.

Vymetalova L, Havlicek L, Sturc A, Skraskova Z, Jorda R, Pospisil T *et al.* (2016). 5-Substituted 3-isopropyl-7-[4-(2-pyridyl)benzyl]amino-1(2)H-pyrazolo[4,3-d]pyrimidines with anti-proliferative activity as potent and selective inhibitors of cyclin-dependent kinases. Eur J Med Chem 110: 291–301.

Weitensteiner SB, Liebl J, Krystof V, Havlicek L, Gucky T, Strnad M *et al.* (2013). Trisubstituted pyrazolopyrimidines as novel angiogenesis inhibitors. PLoS One 8: e54607.

Wesierska-Gadek J, Krystof V (2009). Selective cyclin-dependent kinase inhibitors discriminating between cell cycle and transcriptional kinases: future reality or utopia? Ann N Y Acad Sci 1171: 228–241.

Zimmermann GR, Lehar J, S (2007). Multi-target therapeutics: when the whole is greater than the sum of the parts. Drug Discov Today 12: 34–42.